The Eurasia Proceedings of Science, Technology, Engineering & Mathematics (EPSTEM)
ISSN: 2602-3199

**The Eurasia Proceedings of Science, Technology, Engineering & Mathematics (EPSTEM), 2022**

**Volume 21, Pages 423-429**

**IConTES 2022: International Conference on Technology, Engineering and Science**

# Prediction of Microhardness Profil of Friction Stir Welded Joints of AA3003 Aluminum Alloy

**Chekalil ISMAIL**
University of Djillali Liabes

**Abdelkader MILOUDI**
University of Djillali Liabes

**Ghazi ABDELKADER**
University of Mascara

**Planche MARIE-PIERRE**
University of Belfort Montbeliard

**Abstract**: Friction stir welding is a recommended green process that can replace other assembly techniques. FSW process reveals good mechanical properties, good corrosion resistance and good economic value. For the purpose to evaluate combinations of operating parameters and estimating the welded joint quality, mathematical relationships were carried out using a design of experiment on three levels of rotational speed, feed rate and tool tilt angle. The models allow micro-hardness prediction in the different FSW joint zones of AA3003 aluminum alloy. The interaction of the factors shows that a decrease in rotational speed, angle of inclination and an increase in feed rate leads to a decrease in temperature and good microhardness. A 'W' shape profile of microhardness was shown cross the section, indicating an efficiency equal to 88% and 79% in the nugget and the heat-affected zone successively, compared to the base metal. Contrary any deviation of welding interval may cause various defect such as tunnel voids, 'kissing-bond' defects and crack-like root flaws.

**Keywords:** Friction stir welding, Mathematical relationships, Microhardness, Aluminum alloy

## Introduction

Friction stir welding is an environmentally friendly process and it worths replace other assembly techniques (Fahimpour et al., 2012; Humberto et al., 2016), due to that researchers have carried out several studies in order to understand the combination of the thermomechanical phenomenon exerted by the tool and the metallurgy of the part to be welded during friction stir welding and their influences on the mechanical behavior (Ji et al., 2020; Kimura et al., 2015; Wang et al., 2015).

As a part of a study, a symmetrical 'W' shape profile of hardness was observed on the FSW joints of AA6061-T6 using a stationary shoulder, where the HAZ has the lowest value, and by getting closer to the weld center this value increase sharply up to reaching the TMAZ zone (Sun et al., 2016). Xu et al. (2009) examined the microhardness of FSW joints in different plate thicknesses of AA2219-O, they indicated that the maximum hardness was on the advanced side of the nugget, they also reported that the up of the weld joint was harder than the bottom in the nugget due to the high temperature and the intense mechanical agitation. In addition, the results show clearly that the temperature increases by increasing the speed and/or decreasing the welding speed as for Abdulstaar et al., (2017). They reported that applying shot peening on the FSW joint of AA6061 generally leads to a hardness enhancement in the string zone, especially in the top surface.

The present paper aims to study the interacting of welding parameters to achieve a good quality of AA3003 FSW joint. As well as developing mathematical models to predict microhardness on the different zone of the FSW joints, the results are done by interacting the following welding parameters; rotation speed, feed rate and tool tilt angle.

## Method

Butt friction stir welding were released on a vertical milling machine using an adequate tool geometry. The FSW was performef on AA3003 aluminium plates with the following dimension: 400*110*2 mm. the specimens were cut by a waterjet machine. The microhardness test were carried out on SHIMADZU HMV-2000.

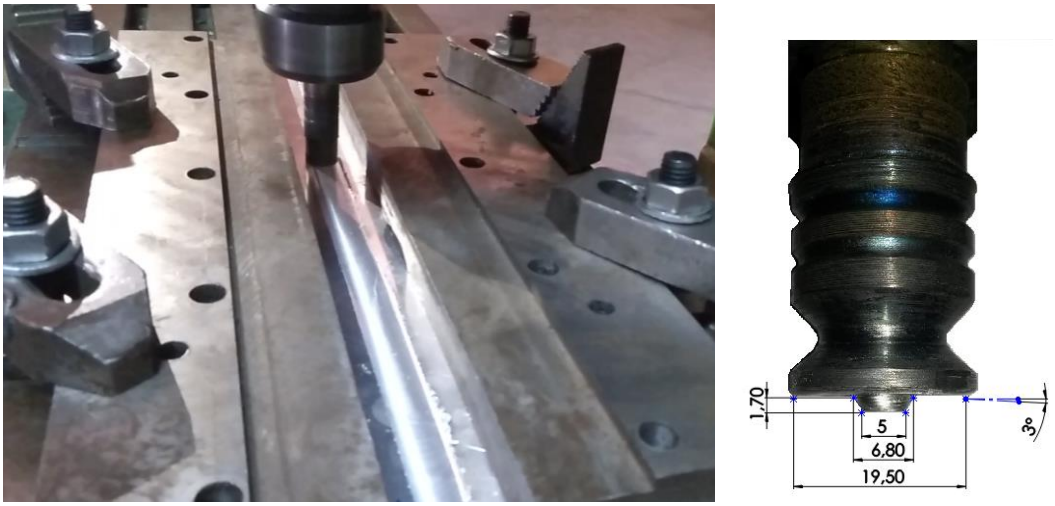


Figure 1. FSW process and the tool geometry


Figure 2. Cutting of specimens

The chemical composition and mechanical properties of the base material before welding are reported in Tabs. 1 and 2. Thechemical composition was obtained by SEM-EDX (Scanning Electron Microscopy - Energy Dispersive X-ray Analysis).

Table 1. Mechanical properties of the material before welding

| Microhardness (HV) | YS (MPa) | UTS (MPa) | RS (MPa) | EL % | YM (GPa) | T Fusion (°C) |
|---|---|---|---|---|---|---|
| 51 | 110 | 160 | 127 | 5.6 | 60 | 650 |

Table 2. Chemical composition of the material before welding

| Element | Al | Mn | Si | Fe | Cu | Ti | Zn | Mg | Cr |
|---|---|---|---|---|---|---|---|---|---|
| % | 96.7 | 1.3 | 0.9 | 0.9 | 0.13 | 0.1 | 0.03 | 0 | 0 |

## Experimental Approach

Figure 3 presents a typical example of the profile obtained during the microhardness test; the important factors of this profil of friction stir welding (FSW) joint profile (Output experimental results) are summarized in Tab. 3.

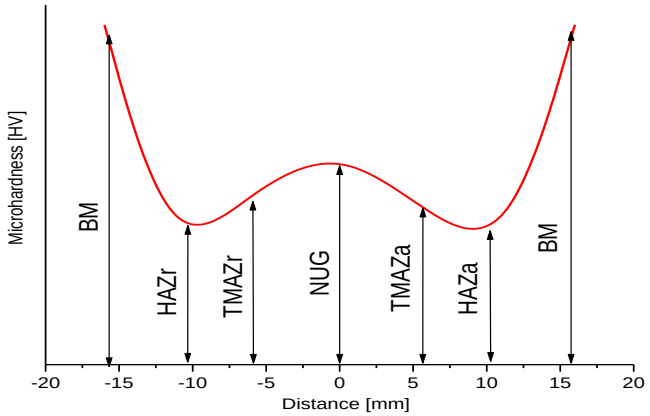


Figure 3. Typical microhardness profil of friction stir welding (FSW) joint

Table 1. Results

| | Facteurs | résultats |
|---|---|---|
| 1 | HAZr | Heat affected zone retreating side |
| 2 | TMAZr | Themomechanicly affected zone retreating side |
| 3 | NUG | nugget |
| 4 | TMAZr | Themomechanicly affected zone advancing side |
| 5 | HAZa | Heat affected zone advancing side |

Table 2. Parameter values for each level

| Parameter | Low level -1 | Central level 0 | High level +1 |
|---|---|---|---|
| Rotation speed (rot/min) | 1000 | 1500 | 2000 |
| Welding speed (mm/min) | 200 | 300 | 400 |
| Tilt angle (°) | 0.5 | 1.5 | 2.5 |

The software MODDE 5.0 (Modeling and Design) [20] is used for the model elaboration and the statistical analysis of the experimental design. If there is curvature in the system, then a polynomial of higher degree must be used, such as the second-order model. The model used has the quadratic form given below:

$$y = a_0 + \sum_{i=1}^{3} a_i x_i + \sum_{1 \le j \le 3} a_{ij} x_j + \sum_{i=1}^{3} a_{ii} x_i^2 + e \qquad (1)$$

$$\boldsymbol{HAZr} = 32{,}67 - 3{,}45.10^{-3}.N + 7{,}15.10^{-2}.S - 1{,}95.T + 4{,}16.10^{-6}.N.S - 5{,}71.10^{-4}.N.T - 4{,}27.10^{-3}.S.T - 2{,}44.10^{-7}.N^2 - 1{,}11.10^{-4}.S^2 + 1{,}37.T^2 \qquad (2)$$

$$\boldsymbol{TMAZr} = 67{,}13 - 2{,}69.10^{-2}.N - 3{,}97.10^{-2}.S - 3{,}8.T + 3{,}87.10^{-6}.N.S + 2{,}33.10^{-3}.N.T - 1{,}97.10^{-3}.S.T + 7{,}04.10^{-6}.N^2 + 6{,}11.10^{-5}.S^2 - 0{,}15.T^2 \qquad (3)$$

$$\boldsymbol{NUG} = 60{,}75 - 1{,}92.10^{-2}.N - 1{,}03.10^{-2}.S - 6{,}39.T + 1{,}11.10^{-5}.N.S + 1{,}06.10^{-3}.N.T - 5{,}95.10^{-3}.S.T + 3{,}86.10^{-6}.N^2 + 6{,}66.10^{-6}.S^2 + 1{,}81.T^2 \qquad (4)$$

$$\boldsymbol{TMAZa} = 53{,}66 - 1{,}27.10^{-2}.N - 2{,}57.10^{-3}.S - 5{,}7.T + 1{,}34.10^{-5}.N.S + 1{,}15.10^{-3}.N.T - 3{,}08.10^{-3}.S.T + 1{,}63.10^{-6}.N^2 - 2{,}33.10^{-5}.S^2 + 1{,}29.T^2 \qquad (5)$$

$$HAZa = 60{,}89 - 2{,}71.10^{-2}.N - 3{,}54.10^{-2}.S - 2{,}36.-3{,}74.10^{-6}.N.+1{,}450766.10^{-3}.N.T - 4{,}56.10^{-3}.S.T + 8{,}23.10^{-6}.N^2 + 8{,}58.10^{-5}.S^2 + 0{,}19.T^2 \quad (6)$$

Table3. Results of the design of experiments tool applied to 30 samples.

| Exp | Des | N [tr/min] | S [mm/min] | T [°] | HAZr [HV] | TMAZr [HV] | NUG [HV] | TMAZa [HV] | HAZa [HV] |
|---|---|---|---|---|---|---|---|---|---|
| 1 | a | 1000 | 200 | 0.5 | 40.45 | 44.16 | 44.66 | 42.34 | 37.85 |
| 2 | b | 1500 | 200 | 0.5 | 34.65 | 37.76 | 38.72 | 41.1 | 32.6 |
| 3 | c | 2000 | 200 | 0.5 | 34.65 | 36.44 | 38 | 36.5 | 34.5 |
| 4 | d | 1000 | 300 | 0.5 | 41.4 | 45.06 | 49.02 | 45.46 | 40.1 |
| 5 | e | 1500 | 300 | 0.5 | 41.4 | 40.04 | 42.84 | 42.14 | 33.4 |
| 6 | f | 2000 | 300 | 0.5 | 35.3 | 38.8 | 44.62 | 37.42 | 37.3 |
| 7 | g | 1000 | 400 | 0.5 | 39.05 | 42.26 | 43.62 | 40.66 | 43.1 |
| 8 | h | 1500 | 400 | 0.5 | 38.7 | 38.24 | 42.02 | 39.6 | 37.1 |
| 9 | i | 2000 | 400 | 0.5 | 37.7 | 40.32 | 44.04 | 40.08 | 37.3 |
| 10 | j | 1000 | 200 | 1.5 | 35.7 | 41.86 | 42.56 | 39.32 | 39.55 |
| 11 | k | 1500 | 200 | 1.5 | 34.75 | 36.86 | 36.18 | 37.34 | 35.5 |
| 12 | l | 2000 | 200 | 1.5 | 34.5 | 41.62 | 36.58 | 33.88 | 35.4 |
| 13 | m | 1000 | 300 | 1.5 | 37.75 | 41.24 | 37.9 | 39 | 33.95 |
| 14 | n | 1500 | 300 | 1.5 | 35.35 | 35.62 | 36.26 | 35.84 | 30.2 |
| 15 | o | 2000 | 300 | 1.5 | 33.2 | 37.76 | 34.76 | 36.84 | 36.05 |
| 16 | p | 1000 | 400 | 1.5 | 39.95 | 37.68 | 42.06 | 37.66 | 37.35 |
| 17 | q | 1500 | 400 | 1.5 | 35.55 | 39.46 | 40.66 | 38.54 | 35.85 |
| 18 | r | 2000 | 400 | 1.5 | 34.35 | 40.28 | 38.5 | 37.96 | 35.05 |
| 19 | s | 1000 | 200 | 2.5 | 41.5 | 36.52 | 42.72 | 40.02 | 33.2 |
| 20 | t | 1500 | 200 | 2.5 | 36.2 | 35.7 | 37.14 | 37.18 | 32.8 |
| 21 | u | 2000 | 200 | 2.5 | 33.85 | 41 | 42.2 | 39.22 | 37.5 |
| 22 | v | 1000 | 300 | 2.5 | 43.6 | 36.08 | 40.72 | 38.36 | 35.8 |
| 23 | w | 1500 | 300 | 2.5 | 41.5 | 34.78 | 41.12 | 38.7 | 32.65 |
| 24 | x | 2000 | 300 | 2.5 | 37.8 | 36.06 | 38.42 | 37.58 | 32.95 |
| 25 | y | 1000 | 400 | 2.5 | 39.15 | 38.7 | 38.06 | 37.64 | 35.85 |
| 26 | z | 1500 | 400 | 2.5 | 37 | 34.1 | 37.28 | 35.7 | 31.15 |
| 27 | aa | 2000 | 400 | 2.5 | 34.75 | 39.58 | 37.96 | 37.4 | 36.25 |
| 28 | bb | 1500 | 300 | 1.5 | 37.75 | 38.18 | 37.82 | 36 | 34.1 |
| 29 | cc | 1500 | 300 | 1.5 | 37.85 | 34.48 | 38.44 | 37.54 | 30.05 |
| 30 | dd | 1500 | 300 | 1.5 | 37.6 | 34.1 | 37.06 | 35.38 | 33.1 |

## Results and Discussion

Generally good quality of the FSW joint has been released at low rotation speed on HAZr. Contrary the low microhardness value was found tilting angle of 1.5° (Figure). In this type of interaction, Hv is large while the two factors S and N take minimal values. Therefore, in order to increase HAZr, it is necessary to decrease S and N. Finally, Figure 4 illustrates the variation of HAZr as a function of the factors T and N. In this case, Hv has high values for two intervals: the first interval corresponds to a rotational speed equal to 1000 rpm and to an angle of inclination Θ comprised between 2.2° and 2.4°, and the second interval corresponds to S comprised between 260 and 400 mm/min and to Θ equal to 0.5° and 2.48°

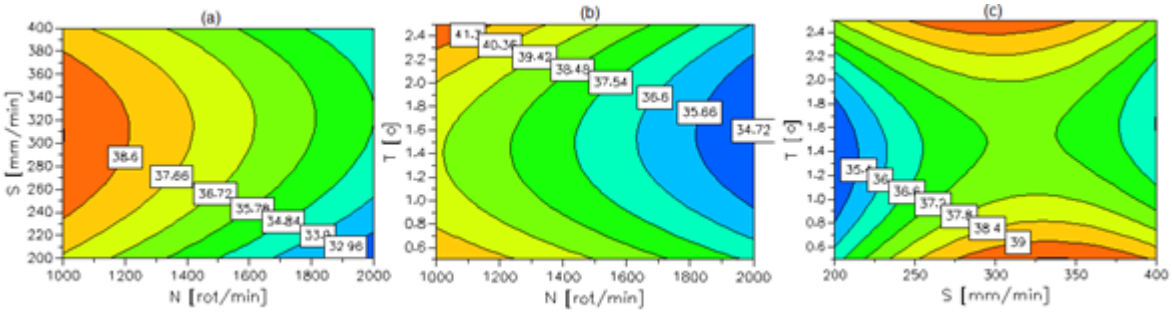


Figure 4. Variation of HAZr as a function of the three factors

Figure 5 presents the effect of the three factors S, T and N acting simultaneously TMAZr The analysis of the graph of this figure suggests that the more N decreases, the more TMAZr also increases until reaching the maximum value of 44 Hv, while S is between [200 and 240 mm/min] and [360 - 400 mm/min]. In addition, it should also be noted that σ_U can reach values closer to the maximum values for a maximum Va equal to 400 mm/min and for a Vr between 1300 and 2000 rpm. In this type of interactions, TMAZr is large while the two factors S and T take minimum and maximum values.

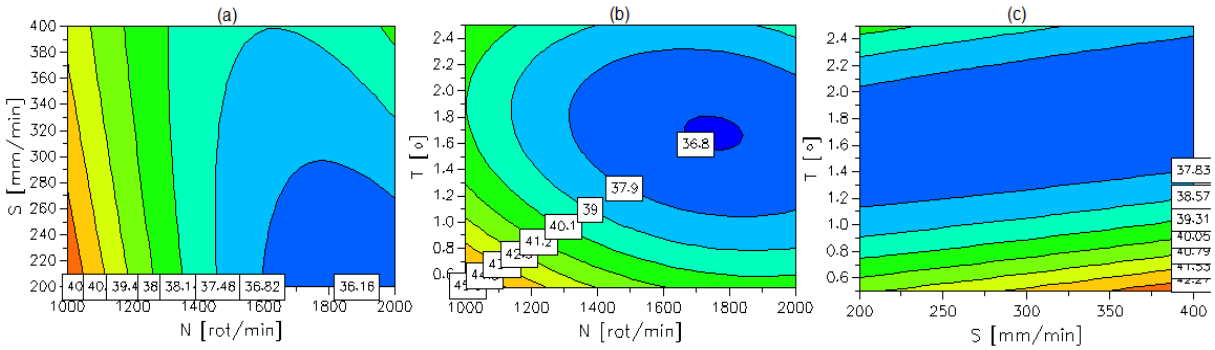


Figure 5 - Variation of nu as a function of the three factors

This new section aims to present the response surface obtained from NU, while varying S and T and N. It can be seen that NU takes maximum values while the two factors S, T and N take minimum values.

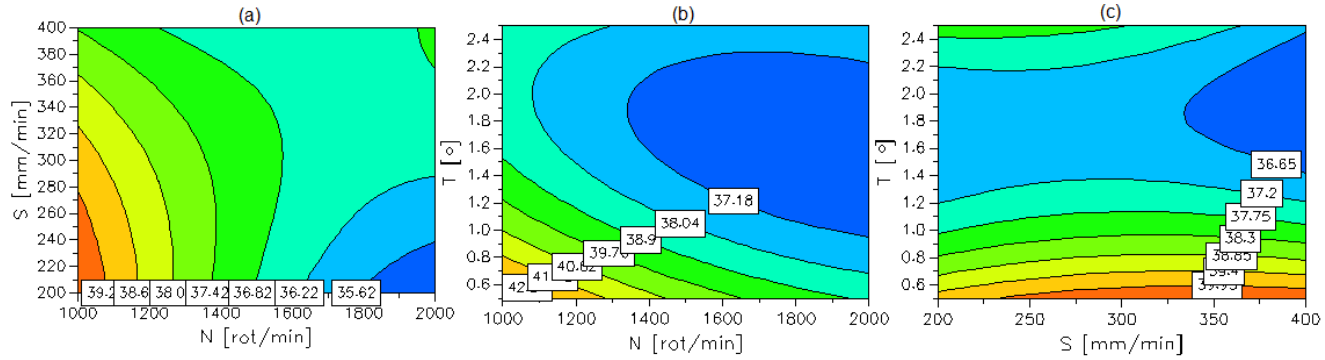


Figure 6 - Variation of tmaza as a function of the three factors

On the other hand, figure 6 illustrates the variation of TMAZa as a function of S, N and T. It can be seen that the simultaneous decrease in S and N leads to an increase in TMAZa; however, increasing S and decreasing T leads to a decrease in TMAZa amplitude. This effect is more pronounced when S is between 250 and 400 mm/min.

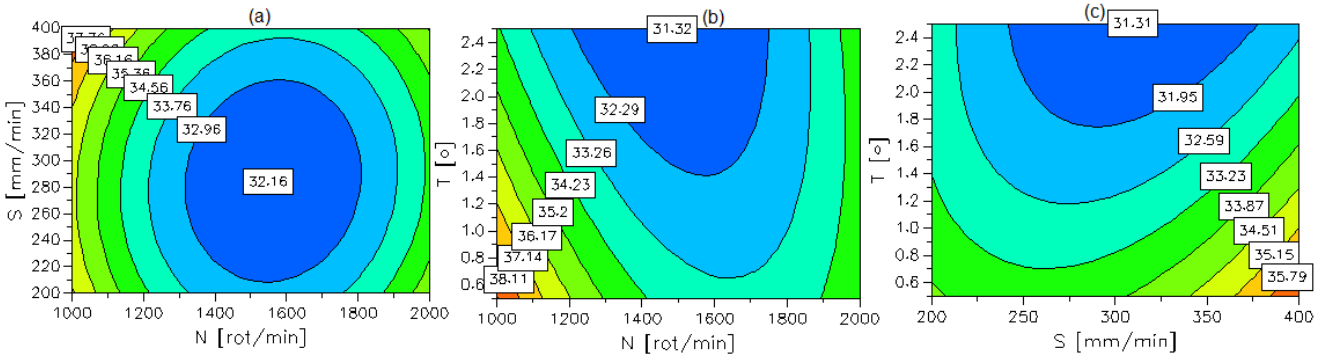


Figure 7.Variation of haza as a function of the three factors

Figure 7 presents the predicted HAZa response as a function of the three factors (S, N and T). Analysis of the curve in this figure shows that a minimum value of HAZa is obtained when the value of Θ is between 1.6 and 2.4°, that of N is in the range of 1300 to 1650 rpm, while S is maintained at 400 mm/min. From these results it is possible to derive the optimum values for the speeds of rotation and the welding speeds. The green curve corresponds to the welding speed 100 mm/min gives optimal results because there is stability on the curve.

From the obtained result (Tab 4) and the previous results we conclude that the decrease in the rotation speed ( high temperature)leads to a good quality of the hardness, this result are in agreement with the founding research of (Tan et al., 2017) , where they prove that increasing in the ambient temperature cause a gradually increase in the recrystallized grains size in the nugget.

Table 4. Optimal values for the mechanical properties of the welded joint

| N [rot/min] | S [mm/min] | T [°] | HAZr [HV] | TMAZr [HV] | NUG [HV] | TMAZa [HV] | HAZa [HV] |
|---|---|---|---|---|---|---|---|
| 1000 | 234.272 | 2.5 | 41.7774 | 36.8592 | 42.3316 | 39.7706 | 34.9224 |
| 2000 | 399.993 | 0.5 | 37.177 | 39.6955 | 42.8259 | 39.8729 | 37.3414 |
| 1000 | 387.525 | 0.5 | 40.7006 | 43.945 | 46.129 | 42.3613 | 41.5184 |
| 2000 | 400 | 2.5 | 34.9685 | 39.385 | 39.6615 | 38.1189 | 35.7396 |
| 1000 | 374.061 | 0.5 | 40.965 | 43.7331 | 46.0729 | 42.539 | 41.0163 |
| 1000 | 227.73 | 0.5 | 39.6441 | 43.7325 | 45.7138 | 43.5942 | 38.7915 |
| 1000 | 315.286 | 0.5 | 41.3575 | 43.2261 | 45.8735 | 43.1556 | 39.4113 |
| 1000 | 387.525 | 0.5 | 40.7006 | 43.945 | 46.129 | 42.3613 | 41.5184 |

## Conclusion

This research focusses on friction stir welding quality in term of microhardness. Microhardness measurement displays W shape profile. Cold welding shows good quality than hot welding. Whatever the welding conditions, there is a decrease in hardness in the HAZ which comes from the restoration. This phenomenon is characterized by the recombination and rearrangement of dislocations leading to a slight decrease in their density. At the limit of the HAZ and TMAZ zones, the granular structure is completely recrystallized and the grains are all equiaxed. At the same time, recrystallization takes place near the TMAZ, resulting in a significant reduction in hardness. In this zone which breaks down into two parts, we find on the HAZ zone side equiaxed grains therefore a recrystallization which is likely to be dynamic and on the core zone side a geometric dynamic recrystallization due to a hot torsion caused by the threading of the rotating pawn. The choice of the operating parameters and the welding mode must therefore be the subject of an in-depth study. It is therefore necessary to define the quality requirements of an FSW weld. The ISO/DIS 25239-3 standard defines the characteristics that the weld beads must comply with in order to validate the choice of operating parameters and the entire welding procedure.

## Scientific Ethics Declaration

The authors declare that the scientific ethical and legal responsibility of this article published in EPSTEM journal belongs to authors.

## Acknowledgements

* This article was presented as an oral presentation at the International Conference on Technology, Engineering and Science ( www.icontes.net ) held in Antalya/Turkey on November 16-19, 2022.

## References

Abdulstaar, M. A., Al-Fadhalah, K. J., & Wagner, L. (2017). Microstructural variation through weld thickness and mechanical properties of peened friction stir welded 6061 aluminum alloy joints. *Materials Characterization, 126,* 64-73.

Fahimpour, V., Sadrnezhaad, S. K., & Karimzadeh, F. (2012). Corrosion behavior of aluminum 6061 alloy joined by friction stir welding and gas tungsten arc welding methods. Materials & Design, 39, 329-333.

Humberto Mota de Siqueira, R., Capella de Oliveira, A., Riva, R., Jorge Abdalla, A., & Sérgio Fernandes de Lima, M. J. W. i. (2016). Comparing mechanical behaviour of aluminium welds produced by laser beam welding (LBW), friction stir welding (FSW), and riveting for aeronautical structures. *Welding International 30*(7), 497-503.

Ji, H., Deng, Y., Xu, H., Lin, S., Wang, W., & Dong, H. (2020). The mechanism of rotational and non-rotational shoulder affecting the microstructure and mechanical properties of Al-Mg-Si alloy friction stir welded joint. Materials & Design, 192, 108729.

Kimura, M., Fuji, A., & Shibata, S. (2015). Joint properties of friction welded joint between pure magnesium and pure aluminium with post-weld heat treatment. Materials & Design, 85, 169-179.

Sun, Z., Yang, X., Li, D., & Cui, L. (2016). The local strength and toughness for stationary shoulder friction stir weld on AA6061-T6 alloy. *Materials Characterization, 111*, 114-121.

Tan, Y. B., Wang, X. M., Ma, M., Zhang, J. X., Liu, W. C., Fu, R. D., & Xiang, S. (2017). A study on microstructure and mechanical properties of AA 3003 aluminum alloy joints by underwater friction stir welding. *Materials Characterization, 127*, 41-52.

Wang, F. F., Li, W. Y., Shen, J., Hu, S. Y., & Dos Santos, J. F. (2015). Effect of tool rotational speed on the microstructure and mechanical properties of bobbin tool friction stir welding of Al–Li alloy. Materials & Design, 86, 933-940.

Xu, W., Liu, J., Luan, G., & Dong, C. (2009). Temperature evolution, microstructure and mechanical properties of friction stir welded thick 2219-O aluminum alloy joints. *Materials & Design, 30*(6), 1886-1893.

## Author Information

**Abdelkader Miloudi**
University of Djillali Liabes, Sidi Bel Abbès, Algeria
BP 89,Sidi Bel Abbès 22000 ,
Algeria
Email: miloudidz@yahoo.fr

**Ismail Chekalil**
University of Djillali Liabes, Sidi Bel Abbès, Algeria
BP 89,Sidi Bel Abbès 22000 ,
Algeria

**Abdelkader Ghazi**
University of Mascara
Bp 305 Route de Mamounia, 29000 Mascara
Algeria

**Planche Marie-Pierre**
University of Belfort Montbeliard
BP 47870, 21078 Dijon Cedex
France

**To cite this article:**

Miloudi, A., Chekalil, I., Ghazi A., & Marie-Pierre, P. (2022). Prediction of microhardness profil of friction stir welded joints of AA3003 aluminum alloy.*The Eurasia Proceedings of Science, Technology, Engineering & Mathematics (EPSTEM), 21*, 423-429.